Zr–LREE rich minerals in residual peraluminous granulites, another factor in the origin of low Zr–LREE granitic melts?

C. Villaseca [a,*], D. Orejana [a], B.A. Paterson [b]

[a] *Department Petrology and Geochemistry, Fac. Geology, Complutense University, 28040, Madrid, Spain*
[b] *Department Earth Sciences, University of Bristol, BS8 1RJ, Bristol, United Kingdom*

Abstract

There is a significant enrichment in some trace elements in the major residual minerals of peraluminous granulite xenoliths from the lower crust. Those trace elements are released from the breakdown of accessory phases at high-T granulite-facies conditions (>850 °C). Around 10 35% of Zr is hosted in granulite rutile and garnet, whereas, the entire LREE Eu budget is controlled by feldspar. The Zr- and REE-compatible behaviour of the major granulite phases, combined with the scarcity of accessory phases, which are mostly included in major granulite minerals, leads to a disequilibrium in accessory dissolution in the peraluminous partial melts. Thus the melt extracts less Zr and LREE and, consequently, generates the false impression of having lower-T when applying current accessory phase dissolution models.

Keywords: Granite petrogenesis; Zr-undersaturation; Residual minerals; Granulites

1. Introduction

Very little is known about the redistribution of REE, Zr and other trace elements during fluid-absent melting under granulite facies conditions, but according to the results of Bea (1996) equilibrium partitioning is rarely attained. Scarce data is available on the trace-element composition of major minerals from granulite facies terranes (e.g. Bea et al., 1994; Fraser et al., 1997) and lower crustal xenoliths (Reid, 1990; Villaseca et al., 2003). Moreover, there has been recent discussion on the apparent existence of low-temperature granitic melts, as indicated by their Zr (and LREE) contents (Miller et al., 2003; Chappell et al., 2004), based on the dependence of zircon (and monazite) solubility on temperature and melt composition during partial melting. This study of the trace-element geochemistry of granulite residua left after the expulsion of granitic melt is designed to move this discussion forward.

We examine the trace-element chemistry of major phases in peraluminous granulite xenoliths from central Spain. They show marked decreases in the abundance of accessory phases with no concomitant depletion in Zr and REE concentrations when compared to equivalent rocks from shallower depths (Villaseca et al., 2001). These lower crustal xenoliths have been interpreted as being the residual keel of the Hercynian peraluminous Spanish Central System (SCS) batholith (Villaseca et al., 1999).

2. Geological setting

Felsic meta-igneous granulites from the SCS have low abundances of the accessory minerals apatite, zircon

* Corresponding author.
E-mail address: granito@geo.ucm.es (C. Villaseca).

and monazite (Villaseca et al., 2003). Most of these granulites also have unzoned almandine-pyrope garnets (Alm_{45-50}–Pyr_{45-55}) (Villaseca et al., 1999). Feldspars show significant ternary solid solution, indicative of high temperature equilibration. Conditions of metamorphism have been estimated at between 850 and 1000 °C, 0.8 to 1.1 GPa, with highly reduced conditions (graphite is common) and very low H_2O partial pressures (Villaseca et al., 1999). Detailed major- and trace-element modelling, combined with isotope (Sr, Nd, O) data, is consistent with the hypothesis that the SCS Hercynian granites were felsic melts in equilibrium with residual granulites of similar composition to the lower crustal xenoliths (Villaseca et al., 1999; Villaseca and Herreros, 2000). Moreover, a recent U–Pb geochronological study on granulite zircons yields an age range of 277 to 312 Ma as the dominant age group, which mainly overlaps with the age of the SCS granite batholith, reinforcing this granulite–granite connection (Fernández Suárez et al., 2006).

Samples from two migmatite terranes have also been included for comparison in this study (100560: a cordierite-bearing anatectic granite from Sotosalbos area, in the SCS, and 93198: a garnet–cordierite-bearing migmatite from the Anatectic Complex of Toledo) (see Villaseca et al., 2001, for further details of the petrography). These are equivalent peraluminous granulite lithotypes to the granulite xenoliths, but represent shallower crustal levels and lower temperatures and pressures of equilibration ($T \leq 800$ °C and $P \leq 0.6$ GPa) (Villaseca et al., 2001).

3. Analytical methods

Concentrations of 24 trace elements (REE, Ba, Rb, Th, U, Nb, Ta, Sr, Zr, Hf and Y) in mineral phases were determined *in situ* on >130 μm thick polished sections by laser ablation ICP-MS (LA-ICP-MS) at the *Department of Earth Sciences* (University of Bristol) using a VG LaserProbe II (266 nm frequency-quadrupled Nd-YAG laser) coupled to a VG Elemental PlasmaQuad 3 ICP-MS. The diameter of the laser spots was approximately 20–30 μm. The counting time for each analysis was typically 100 s (40 s measuring gas blank to establish the background and 60 s for the remainder of the analysis). The NIST 610 and 612 glass standards were used to calibrate relative element sensitivities for the analyses of the silicate minerals. Each laser analysis used Si (or Ca) as an internal standard, with concentrations determined by electron microprobe. Ti was the internal standard for rutile analyses.

Major element mineral compositions were determined at the *Centro de Microscopía Electrónica "Luis Bru" (Complutense University of Madrid)* using a JEOL JXA-8900M electron microprobe with four wavelength dispersive spectrometers. Analyses were performed with an accelerating voltage of 15 kV and an electron beam current of 20 nA, with a beam diameter of 5 μm. Elements were counted for 10 s on the peak and 5 s on each of two background positions. Corrections were made using the ZAF method.

4. Zr-rich rutiles and garnets

Tables 1 and 2 list averaged trace-elements contents of rutile and garnet, respectively, and chondrite-normalized REE patterns for garnet are given in Fig. 1a.

Rutile is the main Ti-bearing phase in SCS granulite xenoliths, which are essentially composed of anhydrous high-T minerals, with Al–Ti-rich phlogopite being scarce or absent (Villaseca et al., 1999). Rutile (modal proportion 1 to 3 vol.%) is an important carrier of Cr and V (up to 4800 ppm and 5400 ppm, respectively) and

Table 1
Average trace element composition of rutile from SCS granulite xenoliths

Sample	U49	105796	95153	U28
	(n=3)	(n=3)	(n=1)	(n=2)
P	123.23	167.47	112.5	113.72
Sc	4.53	50.64	4.84	29.33
V	5422	4163	3084	2285
Cr	1097	1130	593.3	4824
Y	0.29	0.93	b.d.l.	b.d.l.
Zr	3338	878	6860	4042
Nb	1228	496	615	1255
La	0.11	0.23	b.d.l.	1.13
Ce	1.14	0.19	b.d.l.	2.08
Pr	b.d.l.	b.d.l.	b.d.l.	0.16
Nd	b.d.l.	0.71	b.d.l.	0.8
Sm	b.d.l.	b.d.l.	b.d.l.	b.d.l.
Eu	b.d.l.	b.d.l.	b.d.l.	b.d.l.
Gd	b.d.l.	b.d.l.	b.d.l.	b.d.l.
Tb	b.d.l.	b.d.l.	b.d.l.	b.d.l.
Dy	b.d.l.	b.d.l.	b.d.l.	b.d.l.
Ho	0.04	b.d.l.	b.d.l.	b.d.l.
Er	b.d.l.	b.d.l.	b.d.l.	b.d.l.
Tm	b.d.l.	0.13	b.d.l.	b.d.l.
Yb	b.d.l.	0.56	b.d.l.	0.65
Lu	b.d.l.	b.d.l.	b.d.l.	0.07
Hf	127.33	34.24	244.2	103
Ta	69.43	23.23	11.08	51.61
Pb	0.26	b.d.l.	b.d.l.	0.4
Th	b.d.l.	b.d.l.	b.d.l.	b.d.l.
U	59.68	b.d.l.	33.35	7.37

b.d.l.=below detection limits.

Table 2
Average trace element composition of garnet

Sample	Xenoliths							Migmatites
	99185b	104395	U-49	105796	95153	95148	77750b	93198b
	(*n*=3)	(*n*=1)	(*n*=5)	(*n*=3)	(*n*=2)	(*n*=5)	(*n*=2)	(*n*=4)
P	403.47	329.20	385.92	303.90	329.45	n.d.	254.55	299.53
Sc	70.93	72.81	69.35	91.60	80.26	n.d.	76.56	94.38
V	357.17	198.70	335.70	239.17	275.75	187.76	137.10	142.57
Cr	345.33	312.90	448.32	404.57	296.00	255.58	138.55	195.26
Rb	1.16	b.d.l.	0.61	b.d.l.	b.d.l.	0.70	b.d.l	1.01
Sr	0.86	b.d.l.	b.d.l.	b.d.l.	b.d.l.	0.25	b.d.l	0.39
Y	142.30	189.90	137.42	194.23	151.40	61.44	177.60	171.37
Zr	119.80	121.90	46.91	39.47	80.08	94.79	83.19	30.11
Nb	n.d	b.d.l.	b.d.l.	b.d.l.	b.d.l.	0.13	b.d.l	0.18
Ba	2.00	b.d.l.	b.d.l.	b.d.l.	0.95	0.78	b.d.l	b.d.l.
La	b.d.l.	b.d.l.	0.10	b.d.l.	b.d.l.	0.11	b.d.l	b.d.l.
Ce	0.52	0.34	0.13	0.31	0.50	0.36	0.42	b.d.l.
Pr	0.36	0.21	0.12	0.23	0.28	0.32	0.19	0.31
Nd	6.42	2.14	1.96	4.19	5.40	5.84	3.90	1.08
Sm	11.40	3.63	7.08	10.57	9.58	10.13	12.08	2.61
Eu	0.22	0.65	0.13	0.27	0.17	0.14	0.31	0.95
Gd	20.53	15.86	17.56	23.98	15.87	11.34	20.97	10.15
Tb	4.07	4.42	3.93	5.17	2.96	1.86	3.49	3.15
Dy	26.93	35.08	27.52	35.17	24.24	11.14	25.54	26.77
Ho	5.63	7.37	5.70	7.85	6.02	2.54	7.12	6.52
Er	15.54	17.82	13.64	20.71	18.16	9.01	23.65	18.73
Tm	2.15	2.56	1.71	3.13	2.77	1.72	4.05	2.75
Yb	16.12	15.32	11.39	21.55	19.49	15.26	28.92	20.35
Lu	2.24	2.23	1.53	3.10	2.68	3.03	4.47	2.78
Hf	2.28	2.00	0.91	0.93	1.73	1.79	1.69	0.78
Ta	b.d.l.	b.d.l.	b.d.l.	b.d.l.	b.d.l.	0.05	b.d.l	b.d.l.
Pb	b.d.l.	b.d.l.	b.d.l.	b.d.l.	b.d.l.	b.d.l.	b.d.l	b.d.l.
Th	b.d.l.	b.d.l.	b.d.l.	b.d.l.	b.d.l.	0.06	b.d.l	b.d.l.
U	b.d.l.	b.d.l.	b.d.l.	b.d.l.	0.10	0.10	b.d.l	b.d.l.

n.d.=not determined.
b.d.l.=below detection limits.

high-field-strength elements (Zr, Hf, Nb, Ta, U). Rutile Nb contents are consistently > 500 ppm and can be up to 1300 ppm. Recently, the Zr content of rutile has been proposed as a potential geothermometer (Zack et al., 2004). In the sampled xenoliths, rutiles have Zr concentrations that range from 850 to 6850 ppm. The

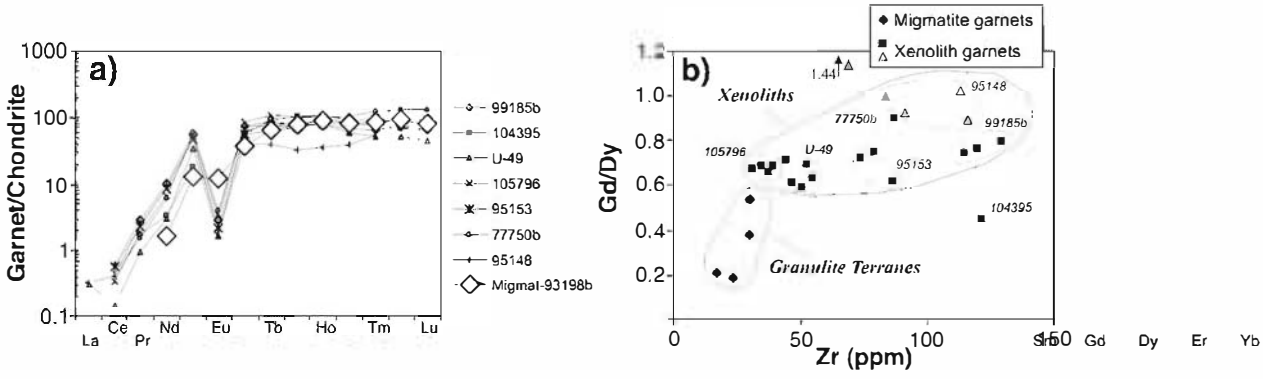

Fig. 1. Chemical features of granulite garnets. a) Chondrite-normalized REE patterns. b) Gd/Dy ratio vs Zr.

rutile thermometer yields temperatures of 850 °C to 1100 °C, slightly higher than estimates from other mineral geothermometers.

Chondrite-normalized REE graphs of the 22 analyzed garnets (Fig. 1a) show a marked negative Eu anomaly (up to 0.02) and an almost flat HREE pattern. The general REE pattern is similar to those found by Reid (1990) in lower crustal peraluminous granulites, but markedly different to those found in garnets from mafic granulitic xenoliths (e.g. Loock et al., 1990). The flat HREE pattern of the garnets is consistent with their lower crustal derivation; the increase in the Gd/Dy ratio has been previously interpreted as being controlled by load pressure (Bea et al., 1997) or zircon/garnet partitioning (Whitehouse and Platt, 2003; Hokada and Harley, 2004). It is interesting to note that all analyzed garnets have MREE (Pr, Nd, Sm) contents higher than chondrite levels, also in agreement with the scarce previous data on felsic granulitic xenoliths (Reid, 1990). Transition metals are also enriched in these granulitic garnets (Cr–V are slightly higher in garnets from the xenoliths than from granulite terranes) (Table 2). Garnets from peraluminous granulites of migmatitic terranes show similar REE contents to those from the granulitic xenoliths (see also Bea et al., 1994; Watt and Harley, 1993), in part due to slightly higher MREE contents in garnets from xenoliths that compensates for slightly lower HREE-Y contents. Thus, the major difference between the two garnet types is HREE fractionation; the Gd/Dy ratio is markedly lower in migmatite garnets (0.28 to 0.40) than those from granulite xenoliths (0.64 to 1.02) (Fig. 1b).

Garnet also has significant Zr contents. Data from the literature show that Zr contents of garnets from peraluminous rocks increase with increasing temperature (Fig. 2). Garnets from felsic peraluminous rocks have the lowest Zr contents under amphibolite-facies conditions (3 to 30 ppm, Schwandt et al., 1996), whereas in outcropping granulite terranes they reach 20 to 65 ppm (Fraser et al., 1997; Degeling et al., 2001). Garnets from peraluminous granulite xenoliths (Condie et al., 2004) and UHT terranes (Hokada and Harley, 2004) have the highest known Zr concentrations (200 to 300 ppm; Fig. 2). Our data are consistent with this pattern; garnets from migmatite terranes have Zr contents <40 ppm, while those from granulitic xenoliths have Zr contents that range from 40 to 130 ppm.

5. LREE-rich feldspars

Table 3 lists averaged trace-elements contents of feldspars whereas their REE patterns are given in Fig. 3.

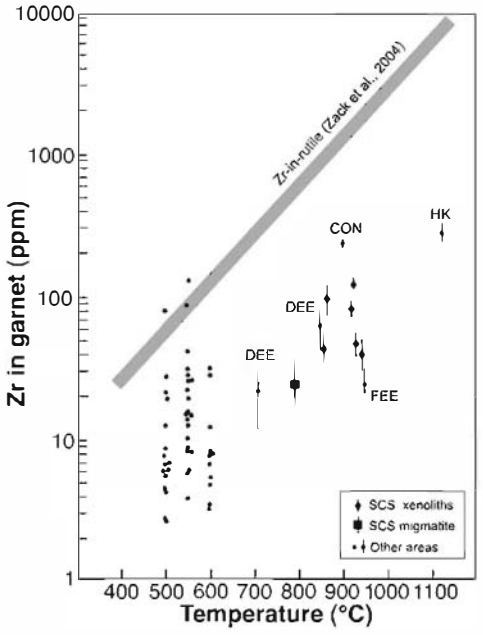

Fig. 2. Zr content in garnet from peraluminous metamorphic rocks vs metamorphic temperature determined from mineral paragenesis. Garnet composition for the lowest temperature range (500 to 600 °C) is taken from amphibolite-facies metapelites (Schwandt et al., 1996). Data for increasing metamorphic grade are taken from DEE (Degeling et al., 2001), FEE (Fraser et al., 1997), CON (Condie et al., 2004) and HK (Hokada and Harley, 2004), mostly in granulite-facies rocks. Garnet compositions for SCS samples are plotted against their estimated geothermometric data (800 °C for Toledo migmatite, Barbero et al., 1995; 850 to 950 °C for granulite xenoliths, Villaseca et al., 1999). The rutile geothermometer of Zack et al. (2004) is included for comparison.

Plagioclase and K-feldspar are abundant (~ 50 vol.%) in the residual SCS felsic granulite xenoliths (Villaseca et al., 1999). Total REE contents in feldspars are usually lower than 100 ppm in most igneous and metamorphic rocks (e.g. Reid, 1990). Feldspars from peraluminous migmatite terranes rarely show REE contents in excess of 100 ppm (e.g. Bea et al., 1994), but some peraluminous granulites in high-T terranes have feldspars with up to 200 ppm total REE (Bea and Montero, 1999). Moreover, peraluminous granulitic xenoliths have feldspars with the highest known REE contents, mostly between 200 and 400 ppm (Reid, 1990; Villaseca et al., 2003; Condie et al., 2004). Our new data corroborate this trend; feldspars from migmatite terranes have total REE contents <80 ppm, whereas those in the granulite xenoliths have higher total REE contents, up to 500 ppm (Fig. 4). Measured REE partition coefficients between plagioclase and K-feldspar in the xenoliths are close to 2, in agreement with empirical studies (Ren et al., 2003; Ren, 2004).

Table 3
Average major and trace element composition of feldspar

Sample	Xenoliths								Migmatites		
Mineral	99185b	U-49	U-49	105796	95153	95148	95148	77750b	100560	100560	93198b
	(*n*=9)	(*n*=3)	(*n*=2)	(*n*=7)	(*n*=6)	(*n*=2)	(*n*=4)	(*n*=2)	(*n*=6)	(*n*=5)	(*n*=7)
	Plg-antiperth	Plg	Antiperthite	Plg	Plg	Plg	Kfs	Kfs	Plg	Kfs	Plg
SiO_2	62.93	62.25	64.23	60.92	61.00	60.06	63.98	64.84	61.99	64.20	59.22
TiO_2	0.04	0.10	0.04	0.03	0.03	0.05	0.04	0.06	0.02	0.00	0.02
Al_2O_3	22.38	22.27	19.67	24.12	24.08	23.38	19.15	18.67	23.88	18.85	25.98
FeO	0.07	0.07	0.04	0.06	0.17	0.07	0.01	0.01	0.05	0.03	0.01
MnO	0.01	0.00	0.00	0.02	0.00	0.00	0.00	0.03	0.01	0.00	0.00
MgO	0.01	0.02	0.03	0.02	0.02	0.03	0.02	0.00	0.00	0.01	0.00
CaO	4.33	5.10	1.44	6.37	6.35	6.22	1.34	0.77	4.52	0.06	6.84
Na_2O	5.54	7.00	3.90	6.83	6.27	6.13	3.46	2.79	8.79	1.49	7.35
K_2O	4.81	1.74	9.42	1.65	1.73	2.11	10.19	11.90	0.36	14.66	0.35
Total	100.12	98.55	98.77	100.02	99.65	98.05	98.19	99.07	99.62	99.30	99.77
Ab	49.9	63.9	35.8	59.7	57.5	55.9	31.7	25.3	76.3	13.4	64.7
An	21.6	25.7	7.3	30.8	32.1	31.4	6.8	3.8	21.7	0.3	33.2
Or	28.5	10.4	56.9	9.5	10.4	12.7	61.5	70.9	2.1	86.3	2.0
P	532	611	676	394	423	n.d.	n.d.	440	389	499	487
Sc	4.73	3.76	3.62	2.47	4.47	n.d.	n.d.	6.95	4.09	4.14	3.05
V	1.34	1.85	0.98	0.71	2.15	1.83	1.01	n.d.	b.d.l.	b.d.l.	1.59
Cr	15.94	13.96	16.71	11.92	14.09	15.94	n.d.	12.53	16.28	15.30	14.33
Rb	84.86	26.62	117	22.69	27.62	50.31	217	273	6.15	365	1.62
Sr	741	474	534	729	603	457	371	294	361	304	526
Y	0.83	1.80	0.26	0.45	8.49	1.44	b.d.l.	8.40	0.50	0.69	1.42
Zr	1.96	1.36	b.d.l.	b.d.l.	9.46	1.45	0.89	3.80	b.d.l.	3.91	b.d.l.
Nb	0.29	b.d.l.	b.d.l.	0.25	b.d.l.	0.21	b.d.l.	b.d.l.	b.d.l.	0.16	b.d.l.
Ba	2577	284	1724	1032	772	673	1918	1766	69.57	3092	63.63
La	92.38	51.64	53.13	67.72	88.75	117.85	73.06	25.27	3.88	1.94	20.72
Ce	151.32	95.75	83.23	118.30	172.30	269.30	126.26	27.81	5.72	2.75	31.20
Pr	14.50	9.57	7.83	11.51	18.20	28.21	11.09	1.57	0.52	0.33	2.54
Nd	49.30	35.04	26.91	41.39	65.82	103.67	34.24	4.56	1.78	2.56	8.24
Sm	4.36	5.26	3.78	4.73	6.40	8.76	2.49	1.31	0.79	0.72	1.64
Eu	5.13	3.49	3.80	4.72	3.91	4.67	4.18	3.82	2.52	2.37	3.73
Gd	1.03	1.68	0.66	1.46	2.00	1.63	0.76	b.d.l.	b.d.l.	b.d.l.	0.95
Tb	0.08	0.15	0.10	0.07	0.28	0.15	b.d.l.	b.d.l.	b.d.l.	b.d.l.	0.11
Dy	0.39	0.51	b.d.l.	0.30	b.d.l.	0.53	0.44	b.d.l.	0.32	b.d.l.	0.44
Ho	b.d.l.	0.21	b.d.l.	0.06	b.d.l.	0.22	b.d.l.	b.d.l.	b.d.l.	0.08	0.08
Er	b.d.l.	0.61	b.d.l.	n.d	b.d.l.	0.16	b.d.l.	b.d.l.	b.d.l.	0.25	b.d.l.
Tm	b.d.l.	0.06	b.d.l.	0.06	0.22	0.10	b.d.l.	b.d.l.	0.08	b.d.l.	b.d.l.
Yb	0.37	0.38	b.d.l.	b.d.l.	b.d.l.	0.26	b.d.l.	b.d.l.	b.d.l.	b.d.l.	0.29
Lu	b.d.l.	0.06	b.d.l.	0.06	b.d.l.	b.d.l.	b.d.l.	b.d.l.	b.d.l.	b.d.l.	b.d.l.
Hf	b.d.l.	b.d.l.	b.d.l.	b.d.l.	0.34	0.15	b.d.l.	b.d.l.	b.d.l.	b.d.l.	0.22
Ta	b.d.l.	b.d.l.	b.d.l.	b.d.l.	b.d.l.	0.08	0.12	0.03	b.d.l.	0.06	b.d.l.
Pb	43.74	29.21	42.57	25.97	32.09	b.d.l.	n.d.	42.90	40.80	107.76	36.49
Th	b.d.l.	b.d.l.	b.d.l.	b.d.l.	0.17	0.20	0.18	b.d.l.	b.d.l.	0.14	b.d.l.
U	0.28	b.d.l.	b.d.l.	b.d.l.	0.07	0.08	b.d.l.	0.09	b.d.l.	0.13	b.d.l.

n.d.=not determined.
b.d.l.=below detection limits.

Chondrite-normalized REE patterns of feldspars from xenoliths show high LREE contents (sometimes close to x400 the chondritic values), with $(La/Lu)_N$ ratios as high as 120 in both alkali-feldspar and plagioclase (Fig. 3). Some plagioclases have slightly higher LREE contents than K-feldspars but similar Eu and HREE contents. Feldspars from migmatite samples have lower LREE contents, but more marked positive Eu anomalies (up to 17) as Eu contents are similar in all analyzed feldspars irrespective of lithology and grade (in the range of 2.4 to 5.3 ppm).

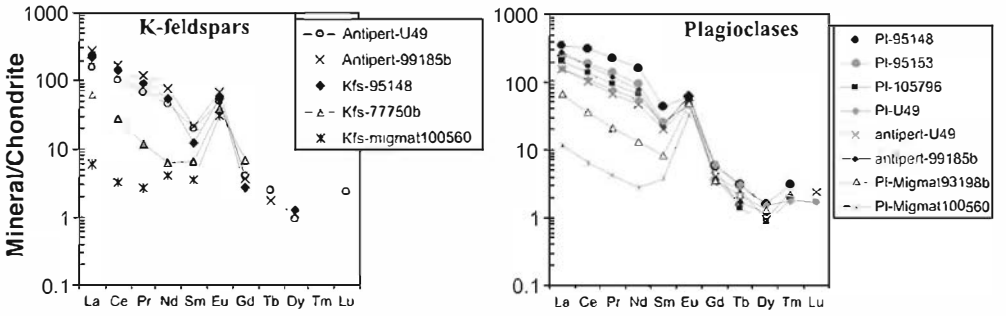

Fig. 3. Chondrite-normalized REE patterns of granulite feldspars.

LREE are more concentrated in those feldspars with greater ternary substitution (Fig. 5) suggesting that crystal chemistry is an important control on feldspar LREE behavior. Plagioclase crystals in SCS granulite xenoliths commonly show antiperthite textures (K-feldspar as ribbons or veins), such that they look like mixed feldspars (Fig. 6a). LREE content increase with increasing Or-molecule in the plagioclase and with increasing (Ab+An)-molecule in K-feldspar, in agreement with data summarized by Ren et al. (2003) and Ren (2004).

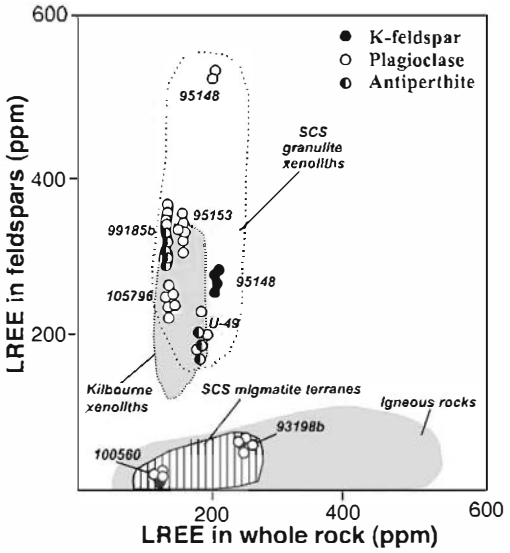

Fig. 4. Total LREE contents in feldspars compared to whole-rock compositions. Feldspars from peraluminous granulite xenoliths show much higher LREE contents (up to 10 times) than feldspars from outcropping peraluminous migmatites (granulite terranes). Other LREE-rich feldspars are from peraluminous granulite xenoliths from Kilbourne Hole (Reid, 1990; Condie et al., 2004). Other feldspars from SCS migmatites (Bea et al., 1994; Villaseca same compositional field. The compositional field from felsic igneous rocks is taken from Reid (1990).

6. Discussion

6.1. REE-Zr mass balance in granulitic xenoliths

Mass balance calculations using whole-rock compositions, mineral trace element data and mineral modes (Fig. 7) show that the SCS felsic granulite xenoliths contrast sharply with felsic magmatic rocks, in which the main mass of the REE and Zr resides in accessory phases. In silicic magmatic rocks, feldspars rarely attain LREE concentrations of greater than 30% of the whole rock concentrations (Reid, 1990). In SCS xenoliths a very large proportion of these trace elements are contained in garnet, rutile and the feldspars, in accordance with scarcity of accessory phases in which these elements are structural constituents (Villaseca et al., 2003).

Garnet is an important host for HREE, Y and Zr, and rutile is a host for Zr, Nb (Ta) and U. The increasing modal proportion of garnet in residual granulites, combined with the breakdown of zircon, monazite and xenotime as metamorphism progresses, promotes this

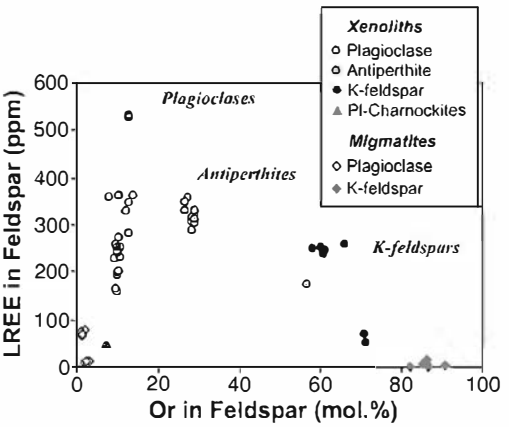

Fig. 5. Correlation between LREE and molecular Or contents in granulitic feldspars (K-feldspar, antiperthitic plagioclase and plagioclase).

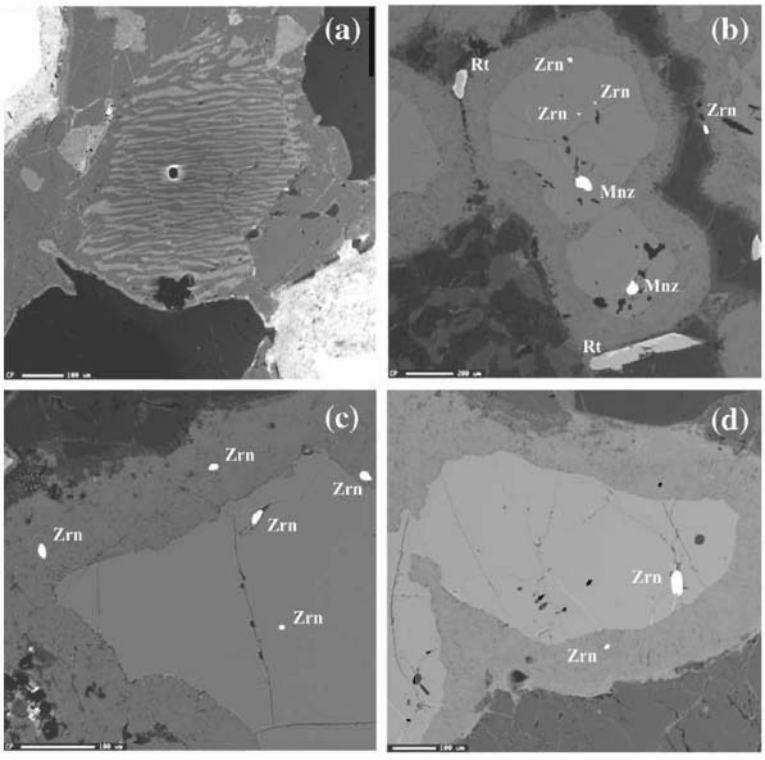

Fig. 6. Back-scatter electron (BSE) images of SCS felsic granulite xenoliths. (a) Antiperthitic plagioclase with K-feldspar in ribbons. See laser ablation pit in the center of the crystal (granulite U-49). (b) Zircon and monazite inclusions in garnet and in their kelyphitic aureola. An intergranular zircon crystal is shown at right (granulite U-49). (c) Zircon inclusions in garnet and in their kelyphitic aureola (granulite 95153). (d) Zircon included in garnet is a larger crystal than zircon in kelyphitic corona (granulite U-49).

Zr-HREE-Y enrichment. Although an average Zr content in garnet of 100 ppm seems relatively low, the high modal proportion of garnet in these xenoliths (mostly 10 to 40 vol.%; Villaseca et al., 1999) suggests that 5 to 10% of the Zr is carried by granulite garnets. Moreover, 10 to 35% of the Zr could be contained in granulite rutiles (Fig. 7). Nevertheless, zircon is always present as an accessory phase in the SCS xenoliths, although its modal proportion is markedly less than in granulites from migmatite terranes (Villaseca et al., 2003). Around 50 to 100% of HREE and Y of the granulite xenoliths are hosted in garnet (Fig. 7). This agrees with recent studies suggesting that HREE are preferentially partitioned into garnet, over zircon, in peraluminous granulites, at high-T conditions (Hokada and Ha ley, 2004).

Feldspars are the major host for LREE and Eu in the peraluminous granulite xenoliths. This enrichment is markedly greater than in the samples from migmatite terranes (Fig. 7). The high modal proportions of feldspar in SCS granulite xenoliths together with the scarcity of monazite (Villaseca et al., 2003), suggests that feldspars control virtually the entire LREE–Eu budget.

6.2. Are low Zr–LREE granites low-T melts?

Zircon and monazite solubility in granitic melts is primarily controlled by temperature and melt composition (Watson and Harrison, 1983; Montel, 1993). Applying accessory mineral saturation thermometry, indicates that most granitic melts are apparently generated at temperatures lower than 840 °C (Miller et al., 2003; Chappell et al., 2004), as granites rarely have more than 300 ppm Zr or LREE. With the exception of A-type granites, most granite suites never reach these high Zr contents.

Experimental phase relationships of granitic rocks indicate liquidus temperatures in the range of 800 to 1000 °C, depending principally on composition and water content. Lower crustal partial melting is essentially H_2O undersaturated (melt H_2O contents <6 wt.%, e.g. Clemens and Watkins, 2001) and low H_2O contents mean higher liquidus temperatures. Experiments by Clemens and Wall (1981) on a peraluminous granite melt with 4 wt.% water (typical of S-type granites) gave a liquidus temperature of more than 900 °C. Shimura et al. (1992) performed crystallization experiments with

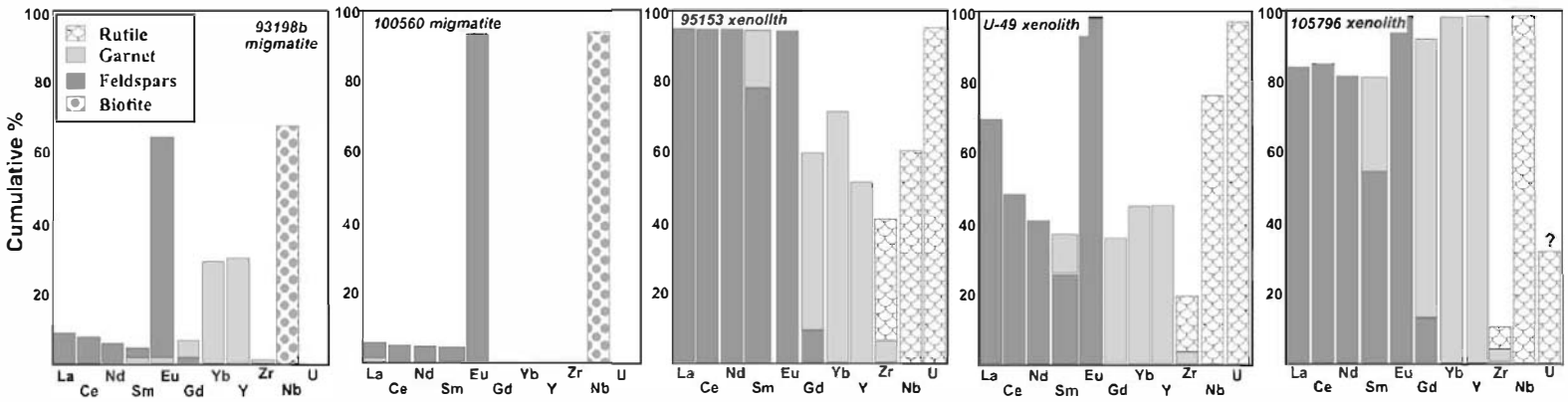

Fig. 7. Relative contributions of the constituent mineral phases to some trace element budgets for samples from migmatites (100560 and 93198b) and lower crustal xenoliths (95153, U-49 and 105796). Migmatite whole-rock compositions used in these mass balance models are taken from Villaseca et al. (2001) (Sotosalbos anatexite n° 1) and Villaseca et al. (2003) (Toledo melanosome 93198). Xenolith chemical analyses are taken from Villaseca et al. (1999) excepting 105796 (La=37.6, Ce=62.8, Nd=24.4, Sm=4.13, Eu=2.11, Gd=4.22, Yb=2.7, Y=26, Zr=157, Nb=3.5, U=0.38, in ppm). Modal compositions as follows: 100560 (Qtz:32, Kfs:19, Pl:26, Bt:10, Crd:7, Sil:0.5), 93198b (Qtz:18, Kfs:17, Pl:15, Bt:21, Crd:22, Grt:5, Sil:0.3), 95153 (Qtz:33, Kfs:10, Pl:39, Phl:2, Grt:15, Rt:1), U-49 (Qtz:30, Kfs:43, Pl:10, Phl:1, Grt:14, Rt:1), and 105796 (Qtz:26, Kfs:3, Pl:42, Grt:15, Opx:11, Rt:1.5). Mineral abbreviations after Kretz (1983).

an S-type tonalite reaching temperatures above 900 °C. These S-type tonalites contained 100 to 150 ppm Zr and applying the Zr saturation thermometer would correspond to a relatively low-T granite of 750 to 795 °C.

Melt inclusion studies on felsic volcanic and subvolcanic rocks give higher temperatures than those estimated by common mineral geothermometry. Most of these melt inclusions give temperatures in the range 850 to 1200 °C (Chabiron et al., 2001) irrespective of peraluminosity. Melt inclusions in plutonic rocks are more difficult to recognize, and they present a significant analytical challenge. Nevertheless, Takenouchi and Imai (1975) describe inclusions in granite porphyries that homogenise mostly in the range 830 to 1100 °C.

To explain this apparent contradiction with experimental and melt inclusion data, Chappell et al. (2004) stated that the generally observed low temperatures, as deduced by accessory dissolution models, imply that granites are not completely molten and, consequently, must contain significant restite.

Migmatite terranes are natural settings in which granitic partial melts are generated, and many of these areas have temperature conditions close to those estimated by accessory phases dissolution models. Migmatitic complexes are common in the inner parts of the Iberian Hercynian Belt. Anatexis in the SCS migmatite terranes occurred mostly in the range of 725 to 825 °C and 0.6 to 0.4 GPa (Barbero et al., 1995; Villaseca et al., 2003). Nevertheless, granitic melts related to these migmatite terranes have major chemical differences when compared to Hercynian granite plutons. Experimental studies on Hercynian metamorphic rocks show that melting below 850 °C rarely produces melt fractions higher than 25 vol.% and these melts are invariably peraluminous leucogranites (Castro et al., 2000). SCS anatectic leucogranites (and leucosomes) are much more SiO_2- and K_2O-rich and CaO-(Na_2O)-, FeO-, MgO- and TiO_2-poor than SCS granitic plutons. The differences are more apparent when trace elements (especially REE and HFSE) are considered. Leucosomes and anatectic leucogranites commonly have low REE contents with marked positive Eu anomalies (Barbero et al., 1995; Villaseca et al., 2001). Restite-rich granitoids from these migmatite terranes are closer in composition to SCS granite plutons, although they show lower CaO (and Na_2O) contents and higher proportions of Cr, Ni and V. These differences suggest that melts generated in the migmatite terranes are unlikely to represent the precursors of SCS granite plutons. Thus, granitic melts generated at these relatively low temperatures (<850 °C) are chemically unlike typical I- and S-type plutons of the SCS.

6.3. SCS residual granulites undepleted in Zr-REE

In accessory dissolution models, the granulitic residue becomes progressively depleted in Zr and LREE as zircon and monazite dissolve in the coexisting granitic melt (Miller et al., 2003). It has been observed that the modal amount of zircon, monazite and apatite decreases dramatically with increasing metamorphic grade (Reid, 1990; Bea and Montero, 1999) and other accessory minerals (e.g. xenotime) are completely consumed before extreme granulite conditions are reached (Villaseca et al., 2003). Nevertheless, SCS granulite xenoliths show Zr and REE contents mostly in the range of 155 to 280 and 120 to 225 ppm, respectively, similar to peraluminous metamorphic rocks from outcropping migmatite terranes. They are not depleted granulites, as would be expected if the accessory phases (zircon and monazite) were mainly dissolved in granitic melts. The mineral chemistry of residual garnets and feldspars in these granulites suggests that a significant proportion of the Zr and REE present in the accessory phases has been transferred to the peritectic mineral assemblage during high-grade metamorphism and/or partial melting (Villaseca et al., 2003). Thus, in the SCS granulite xenoliths there has been growth of Zr-bearing phases (garnet and rutile) and LREE-bearing phases (feldspars) after partial resorption of zircon and monazite. The net result of this competition between granitic melt and residual minerals, for the capture of Zr–LREE, has maintained the respective trace-element composition of the residual solid and the coexisting mobile melt.

Experimental and empirical partition coefficients for feldspars suggest generally incompatible behaviour for the REE. Nevertheless, D_{LREE} in feldspars increases with temperature, as a function of feldspar composition (increasing Ab component in alkali feldspar, and Or in plagioclase), and with melt peraluminosity (Ren et al., 2003; Ren, 2004). Recent data on partitioning between feldspars and peraluminous silicic melts show that D_{LREE} values are invariably <0.5 (mostly 0.1 to 0.3) (Ren et al., 2003; Ren, 2004). Using these D values, granitic melts in equilibrium with LREE-rich residual granulitic feldspars should have La and Ce contents of around 1100 ppm and 4000 ppm, respectively, an order of magnitude higher than typical REE contents in SCS Hercynian peraluminous granites (La: 25 to 50 ppm, Ce: 60 to 105 ppm; Villaseca et al., 1998).

Similarly, empirical D_{Zr} in garnet is in the range of 0.3 to 0.5 (e.g. Koepke et al., 2003), which would yield estimated Zr contents of 100 to 450 ppm in coexisting granitic melts, slightly higher than Zr concentrations

range found in SCS Hercynian granites (typically 125 to 180 ppm; Villaseca et al., 1998).

Accessory dissolution models and empirical solid/melt equilibrium partition coefficients suggest that Zr–LREE-rich peraluminous granitic rocks should be much more common. The fact that they are not could be explained by more compatible behaviour of Zr in garnet and LREE in feldspars in granulitic residua. This would explain why peraluminous felsic melts seldom reach "saturation values" in these trace elements and why granulitic residua are not depleted in these elements.

6.4. Availability of accessory phases in residual granulites and factors leading to Zr-undersaturated peraluminous melts

Although accessory minerals are modally diminished with increasing high-T metamorphism, they still remain in residual granulites (Villaseca et al., 2003). Modal zircon decreases more moderately than monazite or xenotime, the latter phase is not present in SCS granulite xenoliths. The reduction in modal zircon in peraluminous granulites between outcropping migmatite terranes and lower crustal xenoliths is approximately 10 to 50% by volume compared to 50 to 95% reduction of modal monazite (Villaseca et al., 2003). Certainly, mass balance in SCS granulite xenoliths suggests that more than 50% of Zr is hosted in zircon, whereas, monazite is rare in granulite xenoliths and does not control LREE partitioning between residua and melt. A detailed petrographic study of the distribution of zircon in granulite xenoliths shows (Table 4) that most of the zircon crystals (>80%) are included in major phases, mostly (between 38 and 77%) in garnet (Fig. 6b, c, d), and consequently they are physically isolated from any interstitial melt. Nevertheless, between 3 and 21% of zircons are interstitial to at least two other minerals (Fig. 6b). Only a minor fraction of granulitic zircons would react with an interstitial granitic melt. Moreover, calculations by Watson (1996) indicate that most of the small zircons (<100 ìm radius) would dissolve in Zr-undersaturated melts within a few thousand of years at temperatures in excess of 800 °C. Thus, the presence of small zircon crystals at grain boundaries in the SCS granulite xenoliths suggests that any coexisting granite melts have been expelled before equilibrium zircon solubility was attained.

Clemens (2003) suggested that kinetics, rather than equilibrium phase relations, govern zircon dissolution in granitic melts. Inherited cores are common in zircons from SCS granulite xenoliths, although they represent <10% of the total modal zircon (Fernández Suárez et al., 2006). Most of the residual cores are preserved in the largest tabular subhedral zircons, but some inherited cores are also preserved in the more common smaller equant zircon grains (Fernández Suárez et al., 2006). Core preservation and the formation of overgrowths on the larger grains at the expense of smaller grains will continue as long as small zircons and melt exist in the system (Nemchim et al., 2001). If the duration of the interval in which the melt is present is short (high melt segregation rate) large zircon grains will preserve residual cores. The unsuccessful removal of inherited cores during partial melting at temperatures exceeding 850 °C suggests that zircon dissolution does not attain equilibrium. The presence of inherited cores in other studies on lower crustal granulite xenolith suites (Chen et al., 1994; Dostal et al., 2005) suggests that this is a common feature.

Table 4
Zircon location in SCS granulite xenoliths (in %)

	Xenolith-type[a]	In Grt	In Kelyph.	(Grt) T[b]	In Qtz–Kfs–Pl–Sil	Interst.[c]	nd
95148	Felsic (2b)	13.5	41.7	55.2	32.7	12.0	156
99185b	Felsic (2b)	26.7	50.0	76.7	20.0	3.3	30
95151	Felsic (2b)	11.8	55.9	67.7	20.6	11.8	34
U-49	Felsic (2b)	45.0	24.9	69.9	16.6	13.6	169
95153	Felsic (2b)	1.6	58.1	59.7	25.8	14.5	62
81846	Opx-felsic (2a)	–	11.0	11.0	71.5	17.5	91
77750b	Metapelitic (3a)	28.6	9.5	38.1	40.5	21.4	42

[a]Following nomenclature of Villaseca et al. (1999). [b]Total zircon hosted in garnet (including kelyphitic coronas). [c]Interstitial zircon. [d]Number of zircons in a 2.5×4 cm thin section.

Zr undersaturation in peraluminous granite melts generated by dehydration melting reactions at granulite-facies conditions (biotite breakdown) is enhanced by high water undersaturation of the partial melt. Estimated H_2O contents of peraluminous melts in KNASH-systems at the average P–T conditions of SCS granulite xenoliths (900 °C and 9 GPa) are <3 wt.% (Holtz and Johannes, 1994), in good agreement with experimental studies (Carrington and Harley, 1995). Peraluminous melts with less than ~2 wt.% H_2O show a dramatic reduction of zircon solubility (Linnen, 2005). The presence of accessory fluorine-Ti-rich phlogopite in the SCS granulite xenoliths is indicative of the low hydrous content of the residual mica (Villaseca et al., 1999).

7. Conclusions

Models of accessory mineral solubility in granitic melts tend to give unrealistically low temperatures for

melting, typically in the range of 740 to 840 °C. In contrast, experimentally determined phase relations indicate that higher temperatures (850 to 1100 °C) are required for typical granitic rocks to be completely molten. Two possible explanations of this apparent contradiction have been proposed recently: i) granitic melts are mainly low-T melts (probably requiring fluid present melting) which prevent complete dissolution of accessories in the protolith (Miller et al., 2003); ii) granites are strictly "partially molten magmas" characterized by the presence of abundant entrained restite (Chappell et al., 2004).

Previously it has been suggested that accessory phase solubility during crustal melting does not reach equilibrium due to dissolution being slower than melt segregation (e.g. Sawyer, 1991; Bea, 1996; Clemens, 2003). In this study, we suggest that granites are high-T melts without significant entrained restitic material. The residual granulitic counterparts of peraluminous granitic melts have major mineral phases (garnet, plagioclase, K-feldspar and rutile) that contain significant concentrations of Zr and LREE. During granulite-facies metamorphism these new residual minerals become progressively enriched in Zr and LREE (at the expense of zircon and LREE-containing accessory minerals). This trace-element compatible behaviour in residual minerals combined with the shielding of accessory minerals prevents Zr–LREE saturation in the coexisting granitic melts. Recent studies show the common Zr undersaturation of S- and I-type granite melts (Kemp et al., 2005).

This leads to the conclusion that lower crustal partial melting and accompanying solid-melt reactions are more complex than hitherto thought. There is an inadequate knowledge of element partitioning in lower crustal granulites prior to and during melting. Bea et al. (1994) have previously suggested compatible LREE behavior in feldspars, with increasing metamorphic grade. Moreover, a marked change in element partitioning between accessory and major phases in xenoliths has been also suggested (Villaseca et al., 2003).

The sequestering of REE and Zr by the primary granulitic minerals diminishes the influence of accessory mineral dissolution on the trace-element compositions of granitic melts at high temperatures. The percolation of melt within a solid residual matrix rich in minerals with a tendency to be geochemically compatible for Zr and LREE reduces the possibility of expelling trace-element saturated granite melts, irrespective whether they were initially close-to-Zr–LREE-saturated or clearly Zr–LREE-undersaturated. This is in agreement with the general absence of Zr and LREE-rich peraluminous granitoids in the SCS Hercynian Batholith (Villaseca and Herreros, 2000).

Acknowledgments

We are grateful to John D. Clemens, Calvin Miller and Fernando Bea for their insightful comments on a previous version of the manuscript. Whilst the authors also thank the editor Stephen Foley and two anonymous reviewers for their constructive comments on this manuscript. This work is included in the objectives of, and supported by, the CGL2004-02515 DGICYT project of the Ministerio de Ciencia y Tecnología of Spain.

References

Barbero, L., Villaseca, C., Rogers, G., Brown, P.E., 1995. Geochemical and isotopic disequilibrium in crustal melting: an insight from anatectic granitoids from Toledo, Spain. J. Geophys. Res. 100B8, 15745–15765.

Bea, F., 1996. Controls on the trace element composition of crustal melts. Trans. R. Soc. Edinb. Earth Sci. 87, 33–41.

Bea, F., Montero, P., 1999. Behaviour of accessory phases and redistribution of Zr, REE, Y, Th, and U during metamorphism and partial melting of metapelites in the lower crust: an example from the Kinzigite Formation of Ivrea.Verbano, NW Italy. Geochim. Cosmochim. Acta 63, 1133–1153.

Bea, F., Pereira, M.D., Stroh, A., 1994. Mineral/leucosome trace-element partitioning in a peraluminous migmatite (a laser ablation-ICP-MS study). Chem. Geol. 117, 291–312.

Bea, F., Montero, P., Garuti, G., Zacharini, F., 1997. Pressure-dependence of rare earth element distribution in amphibolite- and granulite-grade garnets. Geostand. Newsl. 21, 253–270.

Carrington, D.P., Harley, S.L., 1995. Partial melting and phase relations in high-grade metapelites: an experimental petrogenetic grid in the KFMASH system. Contrib. Mineral. Petrol. 120, 270–291.

Castro, A., Corretgé, L.G., El-Biad, M., El-Hmidi, H., Fernández, C., Patiño Douce, A.E., 2000. Experimental constraints on Hercynian Anatexis in the Iberian Massif, Spain. J. Petrol. 41, 1471–1488.

Chabiron, A., Alyoshin, A.P., Cuney, M., Deloule, E., Golubev, V.N., Velitchin, V.I., Poty, B., 2001. Geochemistry of the rhyolitic magmas from the Streltsovka caldera (Transbaikalia, Russia): a melt inclusion study. Chem. Geol. 175, 273–290.

Chappell, B.W., White, A.J.R., William, I.S., Wyborn, D., 2004. Low- and high-temperature granites. Trans. R. Soc. Edinb. Earth Sci. 95, 125–140.

Chen, Y.D., O'Reilly, S.Y., Kinny, P.D., Griffin, W.L., 1994. Dating lower crust and upper mantle events: an ion microprobe study of xenoliths from kimberlitic pipes, South Australia. Lithos 32, 77–94.

Clemens, J.D., 2003. S-type granitic magmas-petrogenetic issues, models and evidence. Earth-Sci. Rev. 61, 1–18.

Clemens, J.D., Wall, V.J., 1981. Origin and crystallization of some peraluminous (S-type) granitic magmas. Can. Mineral. 19, 111–132.

Clemens, J.D., Watkins, J.M., 2001. The fluid regime of high-temperature metamorphism during granitoid magma genesis. Contrib. Mineral. Petrol. 88, 354–371.

Condie, K.C., Cox, J., O'Reilly, S.Y., Griffin, W.L., Kerrich, R., 2004. Distribution of high field strength and rare elements in mantle and lower crustal xenoliths from the southwestern United States: the role of grain-boundary phases. Geochim. Cosmochim. Acta 68, 3919–3942.

Degeling, H., Eggins, S., Ellis, D.J., 2001. Zr budgets for metamorphic reactions, and the formation of zircon from garnet breakdown. Mineral. Mag. 65, 749–758.

Dostal, J., Keppie, J.D., Hamilton, M.A., Aarab, E.M., Lefort, J.P., Murphy, J.B., 2005. Crustal xenoliths in Triassic lamprophyres dykes in western Morocco: tectonic implications for the Rheic Ocean suture. Geol. Mag. 142, 159–172.

Fernández Suárez, J., Arenas, R., Jeffries, T.E., Whitehouse, M.J., Villaseca, C., 2006. A U–Pb study of zircons from a lower crustal xenolith of the Spanish Central System: a record of Iberian lithospheric evolution from Neoproterozoic to the Triassic. J. Geol. 114, 471–483.

Fraser, G., Ellis, D., Eggins, S., 1997. Zirconium abundance in granulite-facies minerals, with implications for zircon geochronology in high-grade rocks. Geology 25, 607–610.

Hokada, T., Harley, S., 2004. Zircon growth in UHT leucosome: constraints from zircon–garnet rare earth elements (REE) relations in Napier Complex, East Antarctica. J. Mineral. Petrol. Sci. 99, 180–190.

Holtz, F., Johannes, W., 1994. Maximum and minimum water contents of granitic melts: implications for chemical and physical properties of ascending magmas. Lithos 32, 149–159.

Kemp, A.I.S., Whitehouse, M.J., Hawkesworth, C.J., Alarcon, M.K., 2005. A zircon U–Pb study of metaluminous (I-type) granites of the Lachlan Fold Belt, southeastern Australia: implications for the high/low temperature classification and magma differentiation processes. Contrib. Mineral. Petrol. 150, 230–249.

Koepke, J., Falkenberg, G., Rickers, K., Dietrich, O., 2003. Trace element diffusion and element partitioning between garnet and andesite melt using synchrotron X-ray fluorescence microanalysis (mu-SRXRF). Eur. J. Mineral. 15, 883–892.

Kretz, R., 1983. Symbols for rock-forming minerals. Am. Mineral. 68, 277–279.

Linnen, R.L., 2005. The effect of water on accessory phase solubility in subaluminous and peralkaline granitic melts. Lithos 80, 267–280.

Loock, G., Stosch, H.G., Seck, H.A., 1990. Granulite facies lower crustal xenoliths from the Eifel, West Germany: petrological and geochemical aspects. Contrib. Mineral. Petrol. 105, 25–41.

Miller, C.F., McDowell, S.M., Mapes, R.W., 2003. Hot and cold granites? Implications of zircon saturation temperatures and preservation of inheritance. Geology 31, 529–532.

Montel, J.M., 1993. A model for monazite/melt equilibrium and application to the generation of granitic magmas. Chem. Geol. 110, 127–146.

Nemchim, A.A., Giannini, L.M., Bodorkos, S., Oliver, N.H.S., 2001. Otswald ripening as a possible mechanism for zircon overgrowth formation during anatexis: theoretical constraints, a numerical model, and its application to pelitic migmatites of the Tickalara Metamorphics, northwestern Australia. Geochim. Cosmochim. Acta 65, 2771–2778.

Reid, M.R., 1990. Ionprobe investigation of rare earth element distribution and partial melting of metasedimentary granulites. In: Vielzeuf, D., Vidal, Ph. (Eds.), Granulites and Crustal Evolution. Kluwer Acad. Publ, pp. 507–522.

Ren, M., 2004. Partitioning of Sr, Ba, Rb, Y, and LREE between alkali feldspar and peraluminous silicic magma. Am. Mineral. 89, 1290–1303.

Ren, M., Parker, D.F., White, J.C., 2003. Partitioning of Sr, Ba, Rb, Y, and LREE between plagioclase and peraluminous silicic magma. Am. Mineral. 88, 1091–1103.

Sawyer, E.W., 1991. Disequilibrium melting and the rate of melt separation during migmatization of mafic rocks from the Grenvillian Front, Quebec. J. Petrol. 32, 701–738.

Schwandt, C.S., Papike, J.J., Shearer, C.K., 1996. Trace element zoning in pelitic garnet of the Black Hills, South Dakota. Am. Mineral. 81, 1195–1207.

Shimura, T., Komatsu, M., Iiyama, J.T., 1992. Genesis of the lower crustal garnet-orthopyroxene tonalites (S-type) of the Hidaka Metamorphic Belt. Trans. R. Soc. Edinb. Earth Sci. 83, 259–268.

Takenouchi, S., Imai, H., 1975. Glass and fluid inclusions in acidic igneous rocks from some mining areas in Japan. Econ. Geol. 70, 750–769.

Villaseca, C., Herreros, V., 2000. A sustained felsic magmatic system: the Hercynian granitic batholith of the Spanish Central System. Trans. R. Soc. Edinb. Earth Sci. 91, 207–219.

Villaseca, C., Barbero, L., Rogers, G., 1998. Crustal origin of Hercynian peraluminous granitic batholiths of central Spain: petrological, geochemical and isotopic (Sr, Nd) constraints. Lithos 43, 55–79.

Villaseca, C., Downes, H., Pin, C., Barbero, L., 1999. Nature and composition of the lower continental crust in central Spain and the granulite–granite linkage: inferences from granulitic xenoliths. J. Petrol. 40, 1465–1496.

Villaseca, C., Martín Romera, C., Barbero, L., 2001. Melts and residua geochemistry in a low-to-mid crustal section (Central Spain). Phys. Chem. Earth 26, 273–280.

Villaseca, C., Martín Romera, C., De la Rosa, J., Barbero, L., 2003. Residence and redistribution of REE, Y, Zr, Th and U during granulite-facies metamorphism: behaviour of accessory and major phases in peraluminous granulites of central Spain. Chem. Geol. 200, 293–323.

Watson, E.B., 1996. Dissolution, growth and survival of zircons during crustal fusion: kinetic principles, geological models and implications for isotopic inheritance. Trans. R. Soc. Edinb. Earth Sci. 87, 43–56.

Watson, E.B., Harrison, T.M., 1983. Zircon saturation revisited: temperature and compositional effects in a variety of crustal magma types. Earth Planet. Sci. Lett. 64, 295–304.

Watt, G.R., Harley, S.L., 1993. Accessory phase controls on the geochemistry of crustal melts and restites produced during water-undersaturated partial melting. Contrib. Mineral. Petrol. 114, 550–566.

Whitehouse, M.J., Platt, J.P., 2003. Dating high-grade metamorphism-constraints from rare-earth elements in zircon and garnet. Contrib. Mineral. Petrol. 145, 61–74.

Zack, T., Moraes, R., Kronz, A., 2004. Temperature dependence of Zr in rutile: empirical calibration of a rutile thermometer. Contrib. Mineral. Petrol. 148, 471–488.